Report

Current Biology

Neurons of rat motor cortex become active during both grasping execution and grasping observation

Highlights

- Rat M1 contains "mirror" neurons responding to grasping execution and observation
- These mirror neurons are highly specific to grasping actions
- Their matching properties are analogous to those observed in primates
- Observation and execution matching systems are evolutionary preserved

Authors

Riccardo Viaro, Emma Maggiolini, Emanuele Farina, Rosario Canto, Atsushi Iriki, Alessandro D'Ausilio, Luciano Fadiga

Correspondence

fdl@unife.it

In brief

Viaro et al. find that the motor cortex of rats contains "mirror" neurons specifically responding during both execution and observation of grasping actions. These cells are very similar to the mirror neurons originally described in primates and demonstrate that observation and execution matching systems are phylogenetically preserved.

Viaro et al., 2021, Current Biology *31*, 4405–4412
October 11, 2021
https://doi.org/10.1016/j.cub.2021.07.054

CellPress

Current Biology

CellPress
OPEN ACCESS

Report

Neurons of rat motor cortex become active during both grasping execution and grasping observation

Riccardo Viaro,[1,2] Emma Maggiolini,[1] Emanuele Farina,[1] Rosario Canto,[1] Atsushi Iriki,[3] Alessandro D'Ausilio,[1,2] and Luciano Fadiga[1,2,4,*]

[1]Department of Neuroscience and Rehabilitation, Section of Physiology, University of Ferrara, 44121 Ferrara, Italy
[2]Center for Translational Neurophysiology, Istituto Italiano di Tecnologia, 44121 Ferrara, Italy
[3]Laboratory for Symbolic Cognitive Development, RIKEN Center for Biosystems Dynamics Research, Kobe 650-0047, Japan
[4]Lead contact
*Correspondence: fdl@unife.it
https://doi.org/10.1016/j.cub.2021.07.054

SUMMARY

In non-human primates, a subset of frontoparietal neurons (mirror neurons) respond both when an individual executes an action and when it observes another individual performing a similar action.[1–8] Mirror neurons constitute an observation and execution matching system likely involved in others' actions processing[3,5,9] and in a large set of complex cognitive functions.[10,11] Here, we show that the forelimb motor cortex of rats contains neurons presenting mirror properties analogous to those observed in macaques. We provide this evidence by event-related potentials acquired by microelectrocorticography and intracortical single-neuron activity, recorded from the same cortical region during grasping execution and observation. Mirror responses are highly specific, because grasping-related neurons do not respond to the observation of either grooming actions or graspable food alone. These results demonstrate that mirror neurons are present already in species phylogenetically distant from primates, suggesting for them a fundamental, albeit basic, role not necessarily related to higher cognitive functions. Moreover, because murine models have long been valued for their superior experimental accessibility and rapid life cycle, the present finding opens an avenue to new empirical studies tackling questions such as the innate or acquired origin of sensorimotor representations and the effects of social and environmental deprivation on sensorimotor development and recovery.

RESULTS AND DISCUSSION

In primates, a subset of neurons located in the premotor,[1–4] inferior parietal,[5] and primary motor[6–8] cortices of macaque monkeys respond both when an individual executes an action and when it observes or hears another individual performing a similar action. Given this matching of the observed actions onto the observer's motor repertoire, these sensorimotor neurons have been referred to as "mirror neurons." Since their discovery in macaques, similar (audio-motor) mirroring mechanisms have been reported in songbirds, possibly reflecting socially driven sensorimotor learning.[9] An extensive amount of work has suggested that the mirror neuron network could play a role in the development of key cognitive functions.[10] In fact, the sensorimotor matching performed by the mirror networks might be central for motor learning by observation.[11] These inferences are based on indirect measures of neuronal recruitment in humans,[12] and because individual neurons can rarely be recorded in humans,[13] non-human primates are still the experimental model of choice to characterize the behavioral function subserved by mirror neurons. However, the experimental life cycle of non-human primates severely reduces the possibility of investigating key open questions, such as those of social interaction and motor learning.[14] In this regard, murine models have long been valued for their superior experimental accessibility, and although some evidence suggests that they might somehow benefit from observational learning,[15] they have never been employed for the study of individual mirror neurons. Rats reach and grasp objects effectively[16] with a movement kinematics that is somehow similar to monkeys and humans.[17] Moreover, regarding prehension movements, they share with primates many similarities in terms of cortical representation, as evidenced by intracortical microstimulation studies.[18–21] Recent studies further showed that Long-Evans rats make efficient use of visual shapes information in a way that is largely tolerant to variation in object appearance[22] and following a human-like strategy.[23] These elements, together with their social nature,[24] suggests that the rat brain could be an interesting substrate for the study of some so-called "high-level functions,"[25] such as the recognition of others' actions.

Here, Long-Evans rats were trained to perform a reach-to-grasp action toward a food pellet (Figures S1A–S1C). They either had to execute that action or observe another rat perform the same task (Figures S1D and S1E). Observation of another animal performing grooming was used as control condition.[2] A video cameras system was used for kinematic recordings, thus assessing the motor behavior, and to verify attentional orienting of experimental animals (Figure 1A). Consequently, statistical analysis during passive action observation epochs was conducted on those trials showing no forelimb movement

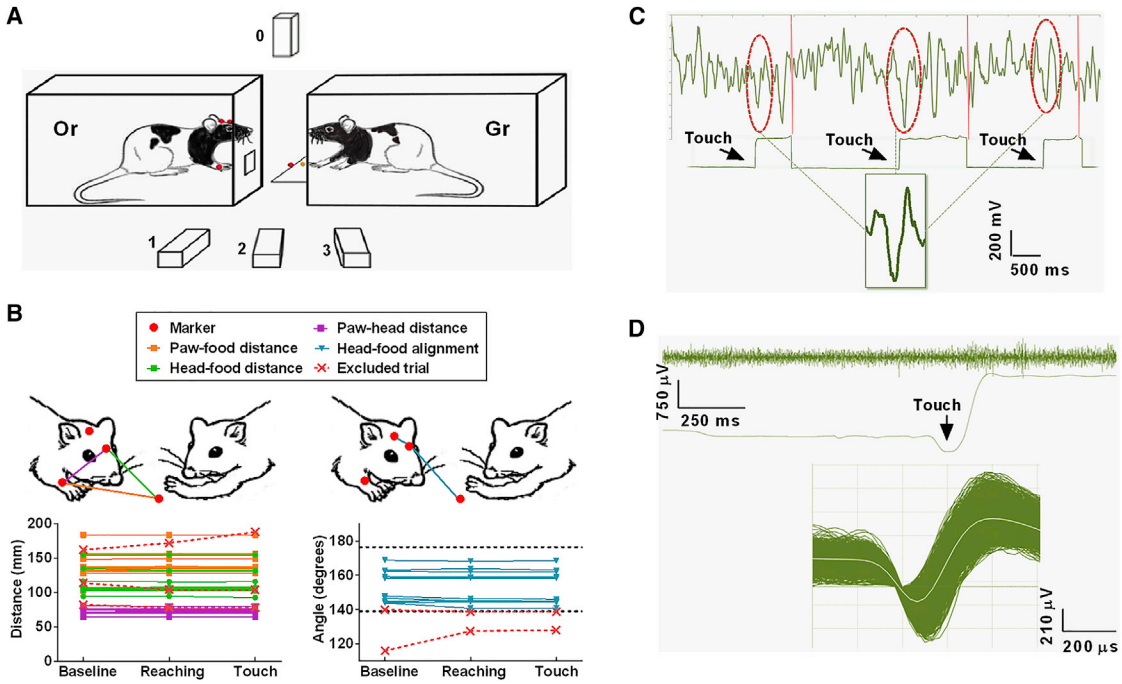

Figure 1. Methodological overview

(A) Schematic view of the experimental setup, with a grasping rat (Gr) and an observing rat (Or), composed by 1–3 infrared cameras and 0 video camera.

(B) Kinematic parameters acquired from a representative "observer" rat at three specific time points. Head-limb (pink), head-food (green), and limb-food (orange) distances and head-food angle (blue) must not exceed cutoff values (dashed black lines). Continuous and dotted colored lines refer to validated and excluded trials, respectively.

(C) Representative segment of µECoG recording, showing three potentials evoked in individual trials and aligned at the touch event (red circles) and the resulting average potential. Red vertical lines indicate end of trials.

(D) Representative segment of intracortical single-neurons recording and superimposed spike waveforms belonging to a single neuron and aligned to the touch event.

See also Figure S1 and Video S1.

as well as aligned head-target line during the three considered time points (baseline and reaching and touch phases; Figure 1B). Epidural field potentials and single-neuron responses of behaving animals were recorded by high-density microelectrocorticography (µECoG) and intracortical recordings from the deep layer V, respectively (Figures 1C and 1D). To define a µECoG site as significantly modulated, the difference in the activity was assessed by unpaired Student's t test between two different 300-ms epochs, namely "baseline" (from 700 to 400 ms before food touch) and "action" (from 150 ms before and 150 ms after touch). To define a neuron as significantly modulated, the difference in activity was assessed by repeated-measures one-way ANOVA followed by Dunnett's post hoc test for multiple comparison among three different 300-ms epochs, namely "baseline" (from 1,000 to 700 ms before food touch), "pre-touch" (from 300 ms before touch to food touch), and "post-touch" (from touch to 300 ms after touch).

Epidural field potentials

µECoG signals were aligned to touch, averaged, and evaluated at the single-electrode level to detect cortical modulations during the different tasks (evoked potentials; Figure 1C). Overall, unpaired Student's t test revealed that 59 recording sites (9.8 ± 1.6 sites per animal) presented a significant modulation. Among these sites, 92% (54/59; 8.9 ± 1.3 per rat) were modulated during grasping execution (motor sites). Of them, 50% (27/54; 4.5 ± 0.9 per rat) showed a significant increase of activity also during action observation (visuomotor sites). The remaining 8% of active sites (5/59; 0.8 ± 0.5 per rat) were modulated only during grasping observation (visual sites). None of the sites responsive to grasping observation responded during grooming observation. The absence of any significant modulation during food presentation allowed us to exclude that the grasping observation-related activation was due to motor preparation or other food-triggered neural processes. Some representative evoked potentials recorded from motor, visuomotor, and visual sites during grasping execution (green profiles), grasping observation (red), grooming observation (blue), and food presentation observation (orange) are shown in Figures 2A–2C. Note that, although motor (Figure 2A) and visual sites (Figure 2C) presented a significant increase of activity around the touch event either during grasping execution or grasping observation, visuomotor sites (Figure 2B) were significantly modulated during both conditions. The representative maps (Figure S1F) and the bi-dimensional, bregma-relative, frequency distribution of execution- and observation-sensitive sites (Figure S1G) showed a consistent topographical organization. In the cumulative maps, motor sites (Figure 2D) were clustered in the forelimb area, prominently in the lateral part of

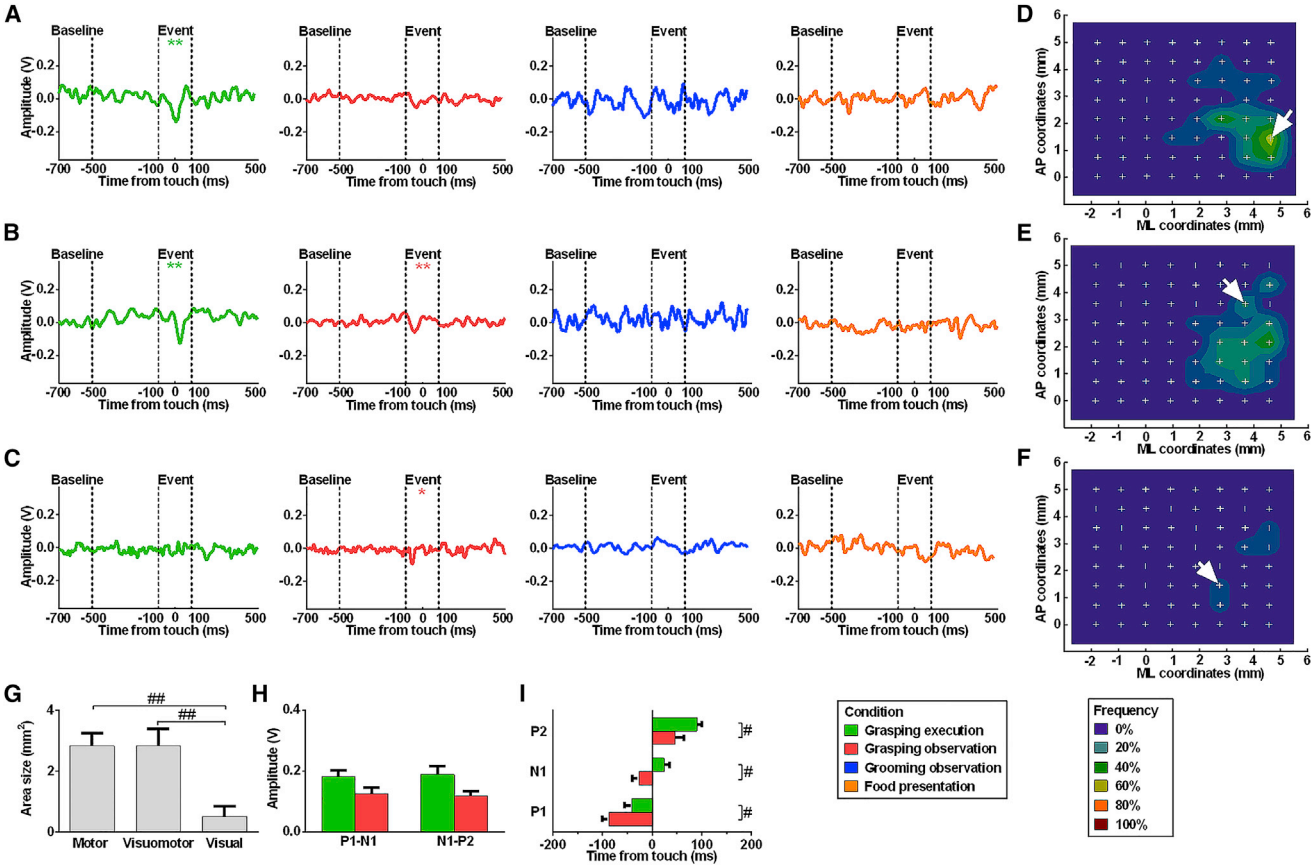

Figure 2. Epidural field potentials

(A–C) Representative μECoG signal of motor (A), visuomotor (B), and visual (C) sites during grasping execution (green), grasping observation (red), grooming observation (blue), and food presentation observation (orange).

(D–F) Frequency color-coded bregma-relative maps of motor (D), visuomotor (E), and visual (F) sites. White arrows on maps indicate the site of the corresponding representative examples.

(G) Area size of motor, visuomotor, and visual sites.

(H and I) Comparison between P1-N1 and N1-P2 amplitudes (H) and P1, N1, and P2 time-to-peak (I) of visuomotor sites during grasping execution and observation.

Data are represented as mean ± SEM. (A–C) $^{**}p < 0.01$ different from baseline. (G–I) $^{\#\#}p < 0.01$ different from other considered conditions. See also Figure S1.

its caudal portion, with visuomotor sites (Figure 2E) largely overlapping the motor ones. By contrast, the few visual sites (Figure 2F) did not clearly cluster within a well-defined region. Accordingly, the one-way ANOVA on the area extension of the motor and visual sites (Figure 2G) revealed a significant difference ($F_{2,15} = 8.80$; $p = 0.0030$). Amplitude and latency of evoked potentials recorded from visuomotor sites were further analyzed (Figures 2H and 2I). Generally, the cortical potential (identified by first positive or P1, first negative or N1, and second positive or P2 peaks) reflects the sequence of cortical recruitment. P1 is the primary evoked potential directly originated from thalamo-cortical connections[26] and may reflect the initial depolarization of layer V that contains pyramidal cells. Following this initial depolarization, axon collaterals produce an enhanced activation which generates the secondary evoked potential N1,[27,28] although P2 arises from the activation of cortico-cortical connections.[29,30] Unpaired Student's t tests showed no statistically significant difference between execution and observation peak-to-peak voltages (Figure 2H) for the P1-N1 ($t_{10} = 1.91$; $p = 0.0857$) and N1-P2 ($t_{10} = 2.21$; $p = 0.0520$) components. The timing of the components (Figure 2I) was significantly different for P1 ($t_{10} = 2.42$; $p = 0.0359$), N1 ($t_{10} = 3.02$; $p = 0.0130$), and P2 ($t_{10} = 2.26$; $p = 0.0470$), with observation-evoked peaks showing shorter latencies. These differences could be due to the presence of different generators in different cortical layers. In fact, when synaptic activity reaches the superficial layers, it propagates horizontally, thus making response latency to increase systematically from more superficial to deeper cortical layers.[31] Thus, this result could be interpreted as based on a laminar dissociation between motor activation for movement generation and motor planning.[32] However, the shorter latency of peaks during observation with respect to execution might reflect a predictive activation pattern,[33,34] because the reaching phase could represent a contextual cue enabling a predictive activation.[35–37] Anyhow, the timing of an evoked potential likely reflects a readout of a coincidence of synaptic transmission in a large population of neurons, without an immediate relation with single-neurons discharge.

Single-neuron activity

μECoG reflects the net activation of a relatively large neural population under the electrode.[38] As a consequence, visuomotor responses can either be expressed by a sub-population of neurons with genuine activation in both conditions or by intermingled unimodal neurons responding either during execution or observation (the same applies to non-invasive recording methods, such as functional magnetic resonance imaging (fMRI), functional near-infrared spectroscopy (fNIRS), magnetoencaphalography (MEG), or electroencephalogram [EEG]). Intracortical single-neuron recordings can disambiguate between these alternative interpretations. We therefore recorded multisite single-neuron activity during action execution and observation from the same regions from where we recorded μECoG potentials, by using a 32-channel microelectrode array connected to a miniature wireless transmitter implanted on the skull of the animals. Signals recorded in each task were aligned to the touch instant as for the μECoG data (Figure 1D). Overall, 158 single neurons were recorded (Figure S1H). Among them, one-way repeated-measures ANOVAs revealed that 152 neurons (25.3 ± 8.7 for each rat) were modulated during grasping execution. Among grasping neurons, 74% (113/152; 18.8 ± 6.9 for each rat) were motor neurons, showing a selective modulation during grasping execution only (motor neurons), whereas 26% (39/152; 6.5 ± 2.3 for each rat) showed a significant increase of spiking activity also during grasping observation (visuomotor neurons). Neurons displaying this dual modulation were observed in each rat, albeit in different proportions. The remaining 4% of neurons (6/158; 1.0 ± 0.6 for each rat) were modulated only during grasping observation (visual neurons). As for μECoG results, none of the neurons responsive to grasping observation responded during grooming observation. Representative motor, visuomotor, and visual neurons recorded during grasping execution, grasping observation, and grooming observation are shown in Figures 3A–3C. Note that, although motor (Figure 3A) and visual (Figure 3C) neurons, respectively, increased their activity during either grasping execution or observation, visuomotor neurons (Figure 3B) showed a significant modulation during both conditions. Other examples of visuomotor neurons recorded from different rats are described in Figures S2A–S2F. In order to define the properties of neurons belonging to the three populations (i.e., motor, visuomotor, and visual neurons), we analyzed the spiking activity recorded during pre-touch (pre-t) (300 ms before touch) and post-touch (post-t) (from food touch to 300 ms after it) epochs. We then compared each condition (action execution, action observation, and grooming observation) against a baseline (from 1,000 to 700 ms before food touch; Figures 3D–3F). Two-way repeated-measures ANOVAs displayed that activity of motor neurons (Figure 3D) showed a significant effect of condition ($F_{2,336}$ = 117.60; $p < 0.0001$) and epoch ($F_{2,672}$ = 45.61; $p < 0.0001$) and a significant condition × epoch interaction ($F_{4,672}$ = 47.24; $p < 0.0001$), justified by the evident increase of their discharge during both pre-t and post-t epochs. By contrast, no significant effect was found for grasping or grooming observation. Firing of visuomotor neurons (Figure 3E) displayed a significant effect of the condition ($F_{2,114} = 93.89$; $p < 0.0001$) and epoch ($F_{2,228}$ = 92.37; $p < 0.0001$) and a significant condition × epoch interaction ($F_{4,228} = 27.68$; $p < 0.0001$) with an increased activity with respect to baseline during both pre-t and post-t epochs. No effect was found for grooming observation. Visual neurons (Figure 3F) displayed a significant effect of condition ($F_{2,15}$ = 16.89; $p = 0.0001$), epoch ($F_{2,30} = 4.46$; $p = 0.0201$), and a significant condition × epoch interaction ($F_{4,30}$ = 10.13; $p < 0.0001$). Post hoc tests confirmed that, for these neurons, during grasping observation, discharge increased with respect to the baseline at both pre-t and post-t epochs. No effect was found for grasping execution or grooming observation, similarly to what was seen on non-human primates.[2] In general, the discharge timing reveals that visual properties are weaker and spread over time, an aspect that is common also in macaques.[39] The bi-dimensional, bregma-relative, frequency distribution of execution- and observation-sensitive neurons (Figure S1I) shows a consistent topographical organization. In the cumulative maps, motor neurons (Figure 3G) appeared clustered in the forelimb area, with a rostro-caudal gradient. Likewise, the distribution of visuomotor neurons (Figure 3H) was almost overlapping, with responsive neurons mainly clustered at coordinates corresponding to the rostral forelimb area and the anterior portion of the caudal forelimb area. By contrast, visual neurons (Figure 3I) show far less spatial specificity. The increased discharge of visuomotor, but not motor, neurons during grasping observation was observed in parallel with an actual immobility of forelimb (Figure S2G). Interestingly, and similarly to what it was originally shown in macaque mirror neurons[1,2] and by the μECoG reported in the present study, grasping observation-related responses of rat visuomotor neurons were unrelated to food presentation. This was demonstrated by both (1) the presence of a statistically significant difference between grasping-related epochs and the baseline (when the food pellet was already visible to the observing rat) and by (2) a further analysis performed on a subset of trials (n = 14) from 9 different neurons/rats where the instant of food placement by the experimenter was occasionally recorded before the starting of the trial (Figure S2H). Although this last analysis was based on a small sample of trials, we consider that the absence of any phasic modulation of neural activity at the instant of food placement, together with the absence of any tonic modulation during food observation by the observing rat, allowed us to exclude that visuomotor responses were "food triggered" or due to "motor preparation." Taken together, these data confirm the hypothesis that the cortical activation during grasping execution and observation was mostly generated by neurons with bimodal sensorimotor properties, mainly expressed in the rostral forelimb area, where complex sequences of reach-to-grasp movement are represented.[19,21,40,41] Accordingly, the rat rostral forelimb sub-region is considered the homologous of the premotor and supplementary motor area of primates,[42] thus playing a key role in conditioning the output of other motor regions.[41] To further discern the specific properties of possible sub-populations, we analyzed the temporal distribution of maximal discharge. Thus, each neuron was classified based on the epoch where its averaged activity was significantly larger, namely pre-t or post-t dominant. In case similar discharge was detected in the two epochs, the neuron was classified as pre/post-t dominant. Considering motor neurons (Figure 3J), a remarkable quantity of neurons were either pre-t dominant (35%; 40/113) or post-t dominant (51%; 57/113), although only a relative small number of cells displayed a pre/post-t dominance (14%; 16/113). Considering visuomotor neurons (Figure 3K), the two most representative

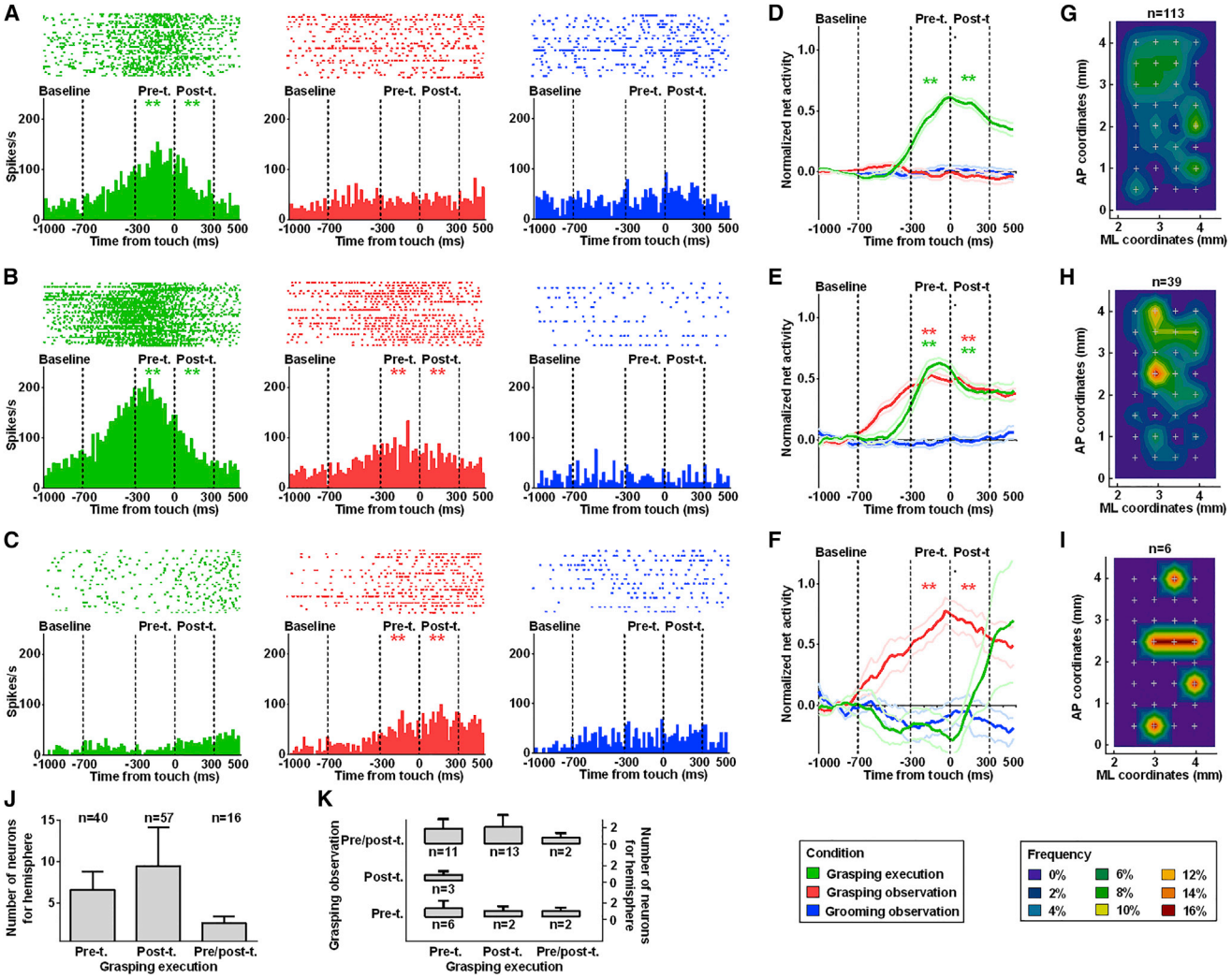

Figure 3. Single-neuron activity

(A–C) Representative discharge of a motor (A), visuomotor (B), and visual (C) neuron during grasping execution (green), grasping observation (red), and grooming observation (blue). Rasters aligned (upper panels) and histograms (lower panels) were considered in specific epochs.

(D–F) Activity of motor (D), visuomotor (E), and visual (F) neuronal populations in the specific epochs.

(G–I) Frequency of discharge, color-coded bregma-relative maps of motor (G), visuomotor (H), and visual (I) neurons.

(J and K) Classification of sub-populations of motor (J) and visuomotor (K) neurons based on epoch dominance. Visuomotor neurons were classified by matching grasping execution and observation.

Data are represented as mean ± SEM. (A–F) **p < 0.01 different from baseline. See also Figures S1–S3.

categories were pre-t or post-t dominant for grasping execution, with a pre/post-t dominance for grasping observation (28%, 11/39 and 33%, 13/39, respectively). A less represented category was constituted by neurons showing a pre-t dominance for both grasping execution and observation (15%; 6/39). Other combinations were only weakly represented (5%–8%; 2–3/39). To characterize the specific properties of these neurons and to verify that they constitute distinct sub-populations, we investigated the averaged activity for motor (Figures S3A–S3E) and visuomotor (Figures S3F–S3J) neurons in relation to their epoch dominance as well as amplitude and time-to-peak activity. In short, results confirmed previous evidence in non-human primates: neurons displaying visuomotor properties share similar discharge timing (relative to the specific phases of grasping movement) of purely motor neurons,[43] although during observation, firing was more spread in time.[44]

At the end of the last recording sessions, to verify that the recording site was effectively the forelimb motor area, somatosensory-evoked potentials (SEPs) were assessed by electrical stimulation of the median nerve of the preferred forelimb, and rough maps were obtained (Figure S3K). Maps revealed significant activation of the caudal portion of the motor cortex, because it receives more afferents compared to the rostral portion,[44] both via direct thalamic projections to primary motor cortex (M1) and by associative connections from primary somatosentory cortex (S1).[45] In addition, visible electrode tracks were examined (Figure S3L). The fact that the electrodes were inserted in the forelimb motor representation until 1,500 μm

below the cortical surface ensures that recordings were performed in layer V of the frontal agranular cortex,[46] supporting the idea that visuomotor activity may originate from pyramidal tract neurons[47] or short-range interneurons modulating them.

Mirror network in rats

In rats, a sequential replay of recent episodes occurred in hippocampus immediately after a motor activity,[48] suggesting an involvement of central areas in the neuronal activation in absence of movements. Accordingly, information reflecting the spatial location of both the self and the other was encoded by hippocampal pyramidal cells in the observer rats.[49] This is in line with the recent observation that the anterior cingulate cortex contains "emotional mirror neurons" responding to the experience of pain and the observation of pain inflicted on other rats.[50] This emotional resonance, similar to that found in single-neuron recordings from a neurosurgery human patient,[51] although supporting the social nature of the rat brain, lacks both the specificity and the effector-related response characterizing the mirror neurons originally described in monkey premotor cortex. Monkey mirror neuron network may act as matching template for others' motor behavior because of the coexistence in the same neurons of visual and motor responses to specific actions. This is what characterizes the visuomotor responses of rat motor cortex we describe here, evoked during both goal-directed actions execution and observation. This finding supports the hypothesis that rats may be provided with a similar neuronal network able to match self and other's experiences. This execution and observation matching system[12] in rats could play a key role in social learning as suggested by the previous finding that rats learn a lever-pressing task faster when they can observe other experienced rats doing the task.[52] Consistently, functional cortical and hippocampal mapping in mice revealed that C-Fos expression increased significantly after the observation of other animals in the swimming task.[53] However, a recent work on mice failed to reveal a mirror response in posterior parietal cortex and secondary motor cortex during the execution and observation of a reaching task.[54] This discrepancy was probably due to different experimental approach, i.e., Ca^{2+} imaging response, and animal conditions, such as forcing attentional state using a head-fixation system.[54] In addition, different from mice, Long-Evans rats are characterized by a highly developed visual system[22] that may play a key role in visuomotor skills as well as in exploratory and social behaviors. In addition, rats motor representations are organized according to discrete ethological[19,21] action maps, rather than simple and discrete movements.[55] Here, we extend this concept to the visual description, and possibly to the identification, of conspecifics' motor acts.

STAR★METHODS

Detailed methods are provided in the online version of this paper and include the following:

SUPPLEMENTAL INFORMATION

Supplemental information can be found online at https://doi.org/10.1016/j.cub.2021.07.054.

ACKNOWLEDGMENTS

This work was supported by University of Ferrara local grants and by Italian Institute of Technology funds to L.F. We thank Dr. A. Casile, P. Cardellicchio, and A. Tomassini for their contribution in writing software parts. We thank Prof. F. Biscarini for his comments on this manuscript.

AUTHOR CONTRIBUTIONS

Conceptualization, L.F.; methodology, R.V. and L.F.; software, R.C.; investigation, R.V., E.M., and E.F.; formal analysis, R.V., E.M., E.F., and L.F.; writing – original draft, R.V. and L.F.; writing – review & editing, R.V., A.I., A.D., and L.F.; funding acquisition, L.F.; supervision, A.I. and F.L.

DECLARATION OF INTERESTS

The authors declare no competing interests.

Received: March 12, 2021
Revised: July 2, 2021
Accepted: July 23, 2021
Published: August 24, 2021

REFERENCES

1. di Pellegrino, G., Fadiga, L., Fogassi, L., Gallese, V., and Rizzolatti, G. (1992). Understanding motor events: a neurophysiological study. Exp. Brain Res. *91*, 176–180.
2. Gallese, V., Fadiga, L., Fogassi, L., and Rizzolatti, G. (1996). Action recognition in the premotor cortex. Brain *119*, 593–609.
3. Umiltà, M.A., Kohler, E., Gallese, V., Fogassi, L., Fadiga, L., Keysers, C., and Rizzolatti, G. (2001). I know what you are doing. a neurophysiological study. Neuron *31*, 155–165.
4. Kohler, E., Keysers, C., Umiltà, M.A., Fogassi, L., Gallese, V., and Rizzolatti, G. (2002). Hearing sounds, understanding actions: action representation in mirror neurons. Science *297*, 846–848.
5. Fogassi, L., Ferrari, P.F., Gesierich, B., Rozzi, S., Chersi, F., and Rizzolatti, G. (2005). Parietal lobe: from action organization to intention understanding. Science *308*, 662–667.
6. Tkach, D., Reimer, J., and Hatsopoulos, N.G. (2007). Congruent activity during action and action observation in motor cortex. J. Neurosci. *27*, 13241–13250.
7. Dushanova, J., and Donoghue, J. (2010). Neurons in primary motor cortex engaged during action observation. Eur. J. Neurosci. *31*, 386–398.

8. Kraskov, A., Dancause, N., Quallo, M.M., Shepherd, S., and Lemon, R.N. (2009). Corticospinal neurons in macaque ventral premotor cortex with mirror properties: a potential mechanism for action suppression? Neuron *64*, 922–930.
9. Prather, J.F., Peters, S., Nowicki, S., and Mooney, R. (2008). Precise auditory-vocal mirroring in neurons for learned vocal communication. Nature *451*, 305–310.
10. Bonini, L., and Ferrari, P.F. (2011). Evolution of mirror systems: a simple mechanism for complex cognitive functions. Ann. N Y Acad. Sci. *1225*, 166–175.
11. Mattar, A.A., and Gribble, P.L. (2005). Motor learning by observing. Neuron *46*, 153–160.
12. Rizzolatti, G., and Craighero, L. (2004). The mirror-neuron system. Annu. Rev. Neurosci. *27*, 169–192.
13. Mukamel, R., Ekstrom, A.D., Kaplan, J., Iacoboni, M., and Fried, I. (2010). Single-neuron responses in humans during execution and observation of actions. Curr. Biol. *20*, 750–756.
14. Colman, R.J. (2018). Non-human primates as a model for aging. Biochim. Biophys. Acta Mol. Basis Dis. *1864* (9 Pt A), 2733–2741.
15. Heyes, C.M., Jaldow, E., Nokes, T., and Dawson, G.R. (1994). Imitation in rats (Rattus norvegicus): the role of demonstrator action. Behav. Processes *32*, 173–182.
16. Whishaw, I.Q., and Coles, B.L. (1996). Varieties of paw and digit movement during spontaneous food handling in rats: postures, bimanual coordination, preferences, and the effect of forelimb cortex lesions. Behav. Brain Res. *77*, 135–148.
17. Sacrey, L.A., Alaverdashvili, M., and Whishaw, I.Q. (2009). Similar hand shaping in reaching-for-food (skilled reaching) in rats and humans provides evidence of homology in release, collection, and manipulation movements. Behav. Brain Res. *204*, 153–161.
18. Graziano, M.S., Aflalo, T.N., and Cooke, D.F. (2005). Arm movements evoked by electrical stimulation in the motor cortex of monkeys. J. Neurophysiol. *94*, 4209–4223.
19. Bonazzi, L., Viaro, R., Lodi, E., Canto, R., Bonifazzi, C., and Franchi, G. (2013). Complex movement topography and extrinsic space representation in the rat forelimb motor cortex as defined by long-duration intracortical microstimulation. J. Neurosci. *33*, 2097–2107.
20. Griffin, D.M., Hudson, H.M., Belhaj-Saïf, A., and Cheney, P.D. (2014). EMG activation patterns associated with high frequency, long-duration intracortical microstimulation of primary motor cortex. J. Neurosci. *34*, 1647–1656.
21. Viaro, R., Bonazzi, L., Maggiolini, E., and Franchi, G. (2017). Cerebellar modulation of cortically evoked complex movements in rats. Cereb. Cortex *27*, 3525–3541.
22. Alemi-Neissi, A., Rosselli, F.B., and Zoccolan, D. (2013). Multifeatural shape processing in rats engaged in invariant visual object recognition. J. Neurosci. *33*, 5939–5956.
23. Rosselli, F.B., Alemi, A., Ansuini, A., and Zoccolan, D. (2015). Object similarity affects the perceptual strategy underlying invariant visual object recognition in rats. Front. Neural Circuits *9*, 10.
24. Kondrakiewicz, K., Kostecki, M., Szadzińska, W., and Knapska, E. (2019). Ecological validity of social interaction tests in rats and mice. Genes Brain Behav. *18*, e12525.
25. Djurdjevic, V., Ansuini, A., Bertolini, D., Macke, J.H., and Zoccolan, D. (2018). Accuracy of rats in discriminating visual objects is explained by the complexity of their perceptual strategy. Curr. Biol. *28*, 1005–1015.e5.
26. Mitzdorf, U. (1985). Current source-density method and application in cat cerebral cortex: investigation of evoked potentials and EEG phenomena. Physiol. Rev. *65*, 37–100.
27. Kulics, A.T., and Cauller, L.J. (1986). Cerebral cortical somatosensory evoked responses, multiple unit activity and current source-densities: their interrelationships and significance to somatic sensation as revealed by stimulation of the awake monkey's hand. Exp. Brain Res. *62*, 46–60.
28. Jellema, T., Brunia, C.H., and Wadman, W.J. (2004). Sequential activation of microcircuits underlying somatosensory-evoked potentials in rat neocortex. Neuroscience *129*, 283–295.
29. Kublik, E., Musiał, P., and Wróbel, A. (2001). Identification of principal components in cortical evoked potentials by brief surface cooling. Clin. Neurophysiol. *112*, 1720–1725.
30. Wróbel, A., Kublik, E., and Musial, P. (1998). Gating of the sensory activity within barrel cortex of the awake rat. Exp. Brain Res. *123*, 117–123.
31. Simons, D.J. (1978). Response properties of vibrissa units in rat SI somatosensory neocortex. J. Neurophysiol. *41*, 798–820.
32. Brown, J.W., Bullock, D., and Grossberg, S. (2004). How laminar frontal cortex and basal ganglia circuits interact to control planned and reactive saccades. Neural Netw. *17*, 471–510.
33. Bonini, L. (2017). The extended mirror neuron network: anatomy, origin, and functions. Neuroscientist *23*, 56–67.
34. Gerbella, M., Rozzi, S., and Rizzolatti, G. (2017). The extended object-grasping network. Exp. Brain Res. *235*, 2903–2916.
35. Kilner, J.M., Vargas, C., Duval, S., Blakemore, S.J., and Sirigu, A. (2004). Motor activation prior to observation of a predicted movement. Nat. Neurosci. *7*, 1299–1301.
36. Fluet, M.C., Baumann, M.A., and Scherberger, H. (2010). Context-specific grasp movement representation in macaque ventral premotor cortex. J. Neurosci. *30*, 15175–15184.
37. Maranesi, M., Livi, A., Fogassi, L., Rizzolatti, G., and Bonini, L. (2014). Mirror neuron activation prior to action observation in a predictable context. J. Neurosci. *34*, 14827–14832.
38. Wang, X., Gkogkidis, C.A., Iljina, O., Fiederer, L.D.J., Henle, C., Mader, I., Kaminsky, J., Stieglitz, T., Gierthmuehlen, M., and Ball, T. (2017). Mapping the fine structure of cortical activity with different micro-ECoG electrode array geometries. J. Neural Eng. *14*, 056004.
39. Kilner, J.M., and Lemon, R.N. (2013). What we know currently about mirror neurons. Curr. Biol. *23*, R1057–R1062.
40. Ramanathan, D., Conner, J.M., and Tuszynski, M.H. (2006). A form of motor cortical plasticity that correlates with recovery of function after brain injury. Proc. Natl. Acad. Sci. USA *103*, 11370–11375.
41. Deffeyes, J.E., Touvykine, B., Quessy, S., and Dancause, N. (2015). Interactions between rostral and caudal cortical motor areas in the rat. J. Neurophysiol. *113*, 3893–3904.
42. Rouiller, E.M., Moret, V., and Liang, F. (1993). Comparison of the connectional properties of the two forelimb areas of the rat sensorimotor cortex: support for the presence of a premotor or supplementary motor cortical area. Somatosens. Mot. Res. *10*, 269–289.
43. Hyland, B. (1998). Neural activity related to reaching and grasping in rostral and caudal regions of rat motor cortex. Behav. Brain Res. *94*, 255–269.
44. Chapin, J.K., and Woodward, D.J. (1986). Distribution of somatic sensory and active-movement neuronal discharge properties in the MI-SI cortical border area in the rat. Exp. Neurol. *91*, 502–523.
45. An, S., Kilb, W., and Luhmann, H.J. (2014). Sensory-evoked and spontaneous gamma and spindle bursts in neonatal rat motor cortex. J. Neurosci. *34*, 10870–10883.
46. Donoghue, J.P., and Wise, S.P. (1982). The motor cortex of the rat: cytoarchitecture and microstimulation mapping. J. Comp. Neurol. *212*, 76–88.
47. Vigneswaran, G., Philipp, R., Lemon, R.N., and Kraskov, A. (2013). M1 corticospinal mirror neurons and their role in movement suppression during action observation. Curr. Biol. *23*, 236–243.
48. Foster, D.J., and Wilson, M.A. (2006). Reverse replay of behavioural sequences in hippocampal place cells during the awake state. Nature *440*, 680–683.
49. Danjo, T., Toyoizumi, T., and Fujisawa, S. (2018). Spatial representations of self and other in the hippocampus. Science *359*, 213–218.

50. Carrillo, M., Han, Y., Migliorati, F., Liu, M., Gazzola, V., and Keysers, C. (2019). Emotional mirror neurons in the rat's anterior cingulate cortex. Curr. Biol. *29*, 1301–1312.e6.

51. Hutchison, W.D., Davis, K.D., Lozano, A.M., Tasker, R.R., and Dostrovsky, J.O. (1999). Pain-related neurons in the human cingulate cortex. Nat. Neurosci. *2*, 403–405.

52. Zentall, T.R., and Levine, J.M. (1972). Observational learning and social facilitation in the rat. Science *178*, 1220–1221.

53. Ushakov, V.L., Kartashov, S.I., Zavyalova, V.V., Bezverhiy, D.D., Posichanyuk, V.I., Terentev, V.N., and Anokhin, K.V. (2013). Network activity of mirror neurons depends on experience. J. Integr. Neurosci. *12*, 35–46.

54. Tombaz, T., Dunn, B.A., Hovde, K., Cubero, R.J., Mimica, B., Mamidanna, P., Roudi, Y., and Whitlock, J.R. (2020). Action representation in the mouse parieto-frontal network. Sci. Rep. *10*, 5559.

55. Graziano, M.S.A. (2016). Ethological action maps: a paradigm shift for the motor cortex. Trends Cogn. Sci. *20*, 121–132.

56. Russell, W.M.S., and Burch, R.L. (1959). The Principles of Humane Experimental Technique (Methuen and Co.).

57. Friedberg, M.H., Lee, S.M., and Ebner, F.F. (1999). Modulation of receptive field properties of thalamic somatosensory neurons by the depth of anesthesia. J. Neurophysiol. *81*, 2243–2252.

58. Tandon, S., Kambi, N., and Jain, N. (2008). Overlapping representations of the neck and whiskers in the rat motor cortex revealed by mapping at different anaesthetic depths. Eur. J. Neurosci. *27*, 228–237.

59. Takano, Y., and Ukezono, M. (2014). An experimental task to examine the mirror system in rats. Sci. Rep. *4*, 6652.

60. Vergara-Aragon, P., Gonzalez, C.L., and Whishaw, I.Q. (2003). A novel skilled-reaching impairment in paw supination on the "good" side of the hemi-Parkinson rat improved with rehabilitation. J. Neurosci. *23*, 579–586.

61. Klein, A., Metz, G.A., Papazoglou, A., and Nikkhah, G. (2007). Differential effects on forelimb grasping behavior induced by fetal dopaminergic grafts in hemiparkinsonian rats. Neurobiol. Dis. *27*, 24–35.

62. Fadiga, L., Caselli, L., Craighero, L., Gesierich, B., Oliynyk, A., Tia, B., and Viaro, R. (2013). Activity in ventral premotor cortex is modulated by vision of own hand in action. PeerJ *1*, e88.

63. Viaro, R., Tia, B., Coudé, G., Canto, R., Oliynyk, A., Salmas, P., Masia, L., Sandini, G., and Fadiga, L. (2017). Finger pressure adjustments to various object configurations during precision grip in humans and monkeys. Eur. J. Neurosci. *45*, 1473–1484.

64. Tia, B., Takemi, M., Kosugi, A., Castagnola, E., Ansaldo, A., Nakamura, T., Ricci, D., Ushiba, J., Fadiga, L., and Iriki, A. (2017). Cortical control of object-specific grasp relies on adjustments of both activity and effective connectivity: a common marmoset study. J. Physiol. *595*, 7203–7221.

65. Viaro, R., Morari, M., and Franchi, G. (2011). Progressive motor cortex functional reorganization following 6-hydroxydopamine lesioning in rats. J. Neurosci. *31*, 4544–4554.

66. Viaro, R., Budri, M., Parmiani, P., and Franchi, G. (2014). Adaptive changes in the motor cortex during and after longterm forelimb immobilization in adult rats. J. Physiol. *592*, 2137–2152.

67. Fan, D., Rich, D., Holtzman, T., Ruther, P., Dalley, J.W., Lopez, A., Rossi, M.A., Barter, J.W., Salas-Meza, D., Herwik, S., et al. (2011). A wireless multi-channel recording system for freely behaving mice and rats. PLoS ONE *6*, e22033.

68. Paxinos, G., and Watson, C. (1982). The Rat Brain in Stereotaxic Coordinates (Academic).

STAR★METHODS

KEY RESOURCES TABLE

REAGENT or RESOURCE	SOURCE	IDENTIFIER
Experimental models: Organisms/strains		
Rattus norvegicus (Long-Evans)	Charles River Laboratories	RRID:RGD_2308852
Software and algorithms		
MATLAB	MathWorks	RRID:SCR_001622
Offline Sorter	Plexon	RRID:SCR_000012
Qualisys Track Manager	Qualisys	N/A

RESOURCE AVAILABILITY

Lead contact

Further information and requests for resources should be directed to and will be fulfilled by the Lead Contact, Luciano Fadiga (fdl@unife.it).

Materials availability

This study did not generate new unique reagents.

Data and code availability

The raw data supporting this study is not available in a public repository because of complex custom data formats and the size of the files but are available from the Lead Contact upon request.

EXPERIMENTAL MODEL AND SUBJECT DETAILS

Subjects

In the present work, twelve adult male Long-Evans rats (Charles River Laboratories), each weighing 250–300 g, were used. During the experiment, animals were housed in individual cages under regular lighting conditions (12 hr light/dark cycle) and temperature/humidity range (21-23°C/55%–65%). The experimental protocol complied with the ARRIVE guidelines and it was designed in compliance with Italian law regarding the care and use of experimental animals (DL26/2014), and approved by the institutional review board of the University of Ferrara and the Italian Ministry of Health (permission n. 332/2015-PR). Adequate measures were taken to minimize animal pain as well as the number of animals used, according to the three Rs principle[56]. For surgery and acute recording procedures, rats were initially anaesthetised with ketamine hydrochloride (80 mg/Kg, i.p.), and supplementary ketamine injections (4 mg/Kg, i.m., given as required, typically every 25–30 min) were used for the duration of the session to maintain long-latency and sluggish hindlimb withdrawal upon pinching the hindfoot (stage III-1 and III-2[57,58]). Under anesthesia, a heat lamp was used to maintain the body temperature at 36–38°C.

METHOD DETAILS

Experimental design

Experiments were aimed at the analysis of motor cortex activation in rats trained to execute a grasping using the forelimb as well as to observe another rat performing the same action. In the first set of experiments, epidural field potentials evoked during the different tasks were evaluated by using 64-channel μECoG arrays positioned over the whole motor cortex. In the second set of experiments, single-neuron discharge during the different tasks was evaluated by using 32-channel intracortical arrays with electrode tips in layer V of the forelimb motor representation. The behavioral sequences to which rats were submitted are schematically described in Figure S1E. After completion of recording sessions, a cortical mapping of potentials evoked by electrical stimulation of the median nerve as well as the histological evaluation were performed to assess electrode sites placement.

Behavioral apparatus

The overall apparatus is similar to that proposed by a recent work[59]. Substantially, it consisted of two identical clear Plexiglas boxes, each measuring 45 cm height × 15 cm width × 35 cm depth, facing each other. This box design is classically employed to investigate the ability of a rat to reach for and grasp a single food pellet[16,60,61]. Two animals were placed in the two different boxes at the same

time, always with the same partner. Each rat had to execute a series of grasping or observe the other rat performing grasping or grooming. Tasks were performed in a random sequence. In order to maintain motivation high, rats were placed on a restricted diet to maintain 90% of normal free-feeding body weight for the duration of experimental procedures (training and recording sessions). At the end of each session, animals were re-housed in their own cage, and rewarded with an extra dose of food pellets. Water was always available *ad libitum*.

Grasping task

Rats were expected to extend their preferred paw to retrieve a rounded food pellet (~45 mg each; TestDiet, Richmond, USA) and the procedure used was similar to that described by previous reports[20]. Rats were trained to do so by extending the forelimb through an aperture (15 cm height × 1 cm width), to grasp and eat one food pellet at a time (Figure 1A). Rats undergoing the skilled reaching task were trained for several days (usually 4 weeks). Following an initial period of grasping using the mouth, the rat was then forced to use its paw. After a few days, rats developed a consistent preference for either the left or right paw during the reaching/grasping phase, but used both paws to bring the food to the mouth and hold it while they ate (manipulation phase). The food pellets were placed in a small indentation on a shelf located outside the slit (3 cm high with respect to the floor of the box). The box was embedded with an infrared sensor placed on the bottom of the indentation, triggering when the food pellet was removed by the grasping rat. Animals were also trained to walk to the rear wall of the box after each attempt, in order to readjust their body position before the next attempt to grasp a pellet. Rats were observed daily and the their performance on 40-60 attempts (usually ~20 min) was determined. During the experiment, each trial started with the removal of a black screen (12 × 12 cm) initially placed in front of the Plexiglas cage of the grasping rat to prevent the vision of the food pellet, previously placed by the experimenter and always visible to the observing rat. The inter-trial interval depended on the individual rat behaviors (usually 20-30 s). Completion of training was defined as five successive sessions in which the rat executed at least 70% successful trials for each task (Figures S1A–S1C).

Grooming task

Rats were routed near the slit by placing one food pellet and few drops of 5% glucose solution were dropped by the experimenter over the face, thus inducing the animal to perform a self-cleaning action using forelimbs. This task did not need training, and a maximum of 10-15 trials per recording session were allowed to avoid stress and/or loss of motivation. The inter-trial interval depended on the individual rat behaviors (usually 30-60 s). In order to maintain high levels of motivation, the rat was rewarded each 3-5 trials with an additional food pellet.

Observation task

Rats had to pay visual attention to the task performed by the other rat (grasping or grooming) maintaining a static posture (Figure S1D). The proximity of the two boxes allowed the rat to view the food pellet to be grasped by the other rat but too far to be reached by the observing rat. In the food presentation condition, the rat had to pay attention to the food alone, placed in the same position used for grasping observation (without the presence of the other rat). The food pellet was presented to the observing rat by the removal of a black screen (12 × 12 cm) placed initially in front of the Plexiglas cage to prevent the vision of the food pellet. The inter-trial interval depended on the individual rat behavior (usually 20-60 s). In order to maintain high levels of motivation, the rat was rewarded each 3-5 trials with an additional food pellet. This task did not need systematic training, since animal attention appeared influenced by several contextual-independent experimental variables.

Trials validation

Trials were considered for analysis only when both acting and observing rats have performed a correct trial.

Grasping task

A trial was scored as correct if a rat obtained the pellet and then consumed it, or if the pellet dropped during retraction. On the contrary, the trial was not considered if the pellet was pushed off the shelf by an imprecise movement.

Grooming task

A trial was scored as correct if a rat performs the self-cleaning in front of the slit. Otherwise, the trial was not considered if the action was performed more than 5 cm away from the slit.

Observational task

Two consecutive steps of validation were used to identify a correct trial. Only trials when the observer rat was motionless in front of the slit during the action performed by other rat were considered for the second step of validation. The second step of validation consisted in a quantitative characterization of immobility and visual attention to the grasping or grooming execution as well as to food presentation. During μECoG recording, an optical 3D motion analyzer (Qualisys Motion Capture System; Qualisys North America Inc, Charlotte, USA), in which the X-, Y- and Z- axes corresponded to the anterior, lateral and dorsal directions, respectively, was used to record the spatial position over-time a of adhesive infrared-reflective spherical markers (weight: 0.04 g, diameter: 0.30 cm) placed on the observer rat (Figures 1A and 1B), through three infrared cameras positioned around the box. This setup was previously employed to evaluate kinematics of ICMS-evoked movements in rats[19–21] as well as grasping in non-human primates[62,63]. To verify the absence of possible forelimb movements, one marker was positioned on the forelimb skin, i.e., the dorsal middle of the wrist. In parallel, to evaluate the visual attentional state, other two markers were positioned on the frontal and the occipital edges of the recording chamber. An additional marker was fixed in the rear of the small indentation for the food pellets (food marker). To minimize positional variability, markers were positioned by the same operator in all experiments. Markers were placed on the rat only during the observational tasks to avoid any possible influence on grasping performance or stress-induction. Recordings were collected at a sampling rate of 100 Hz and Qualisys Track Manager software was used to calculate kinematic features offline (Video S1). During

intracortical recording, since the chronic implant was performed by fixing the multi-electrode array directly on the skull without a recording chamber, an optimal positioning of the infrared reflective markers was not possible. Thus, two video cameras were positioned around the Plexiglas box of the observer rat to obtain a lateral and a dorsal view of the animal and its behavior was videotaped at 60 frames/s. Both dorsal and lateral views were evaluated offline frame-by-frame using commercial free softwares (VirtualDub: https://www.virtualdub.org and Avidemux: http://fixounet.free.fr/avidemux), virtual markers being positioning manually by the experimenter at the salient frames. On both motion capture data, we first evaluated head and forelimb proximity to the aperture and motionless by measuring reciprocal distances between three markers, namely that positioned on the rostral part of the chamber, wrist and food pellet (Figures 1A and 1B). A displacement below 5% of the distance at baseline lead a trial validation. We then analyzed head-food alignment to verify if the rat was paying attention to the task (grasping and grooming). The amplitude of the angle formed by the virtual axis passing through the two head markers and that passing through the rostral marker of the head and food, was evaluated (Figure 1B). An angle comprised in the range 139.1-176.5 degrees (for the infrared system) or 170.0-190.0 and 152.5-179.8 degrees (respectively, for top and lateral views of video cameras system) lead at trial validation. For a trial to be valid, the head-food angle must be comprised between two pre-selected cut-off values (horizontal dashed lines in Figure 1B). Cut-off values were derived from the grasping condition, where the animal is facing toward the food being its visual attention directed toward the to-be-grasped target. Trials showing a marker displacement or unaligned position of the head-food markers during at least one of the three considered frames, namely baseline (frame at 500 ms before touch), reaching (frame in which the paw comes out from box aperture) and touch (frame corresponding at the beginning of food grip) was excluded from further analyses. Considering grooming observation, the same criteria were used. Reciprocal distances of forelimb and head were measured to assess immobility. Proximity of the two animals and the virtual axis passing between the two head markers was used to verify that attention was directed toward the rat performing the grooming action.

Surgical procedures

After the end of training, ketamine-anaesthetised rats were placed in a Kopf stereotaxic apparatus (David Kopf Instruments, Tujunga, CA, USA). A craniotomy was performed to expose the frontal cortex of the hemisphere contralateral to the preferred limb. Each underwent different procedures depending on whether they were going to be used for recording epidural field potentials or single unit activity. After surgery, each rat was re-housed in their cage and treated with analgesic and antibiotic drugs until complete recovery (usually two or three days).

Epidural field potentials

The dura remained intact and kept moist with saline. A custom-made titanium recording chamber (18 mm length, 13 mm wide and 12 mm height) was surgically implanted on the selected hemisphere. The chamber was fixed to the skull using screws and dental cement (Jet Repair Acrylic; Lang Dental Manufacturing, Chicago, IL, USA). Using a micromanipulator (David Kopf Instruments, Tujunga, CA, USA), a custom-made flexible 8 × 8 μECoG array[64], measuring 7 mm in the ML × 8 mm in the AP direction, was inserted within the chamber and placed over exposed cortex. The 63 active electrodes are in gold (impedance: 0-5-1.5 MΩ at 1 KHz) with a contact diameter of 0.1 mm and inter-electrode distance of 0.9 mm in the ML and 0.7 mm in the AP direction. The size of the array ensure that the whole motor cortex is recorded, thus including the vibrissa and forelimb motor representations of the selected hemisphere. An electrode located in the angle of the array served as reference. Finally, the array was blocked through its connectors (Omnetics Connector Corporation, Minneapolis, USA) to the chamber with a cover.

Single neuron activity

Under surgical stereomicroscopy (Carl Zeiss Meditec AG, S100/OPMI pico, Jena, Germany), the dura was removed and the cortex kept moist with saline. Using a micromanipulator, a 4 × 8 intracortical arrays (MEA, Microprobes, Gaithersburg, USA) measuring 1.5 mm in the ML × 3.5 mm in the AP direction, was lowered vertically to 1500 μm below the cortical surface, corresponding to layer V of the frontal agranular cortex, in the area comprised between 2.5-4.0 mm in the ML and 0.5-4 mm in the AP direction, that usually constitutes the forelimb representation[21,65,66]. The 32 active electrodes were in platinum-iridium (impedance: 0.5-1.5 MΩ at 1 KHz) with an inter-electrode distance of 0.5 mm in the ML and AP direction. Array dimensions ensure that the whole forelimb representation was recorded. A screw implanted more caudally with respect the craniotomy served as reference. After electrode implantations the exposed cortex was covered by silicone elastomer Kwik-Cast (Word Precision Instruments, Sarasota, USA). Finally, the array was fixed to the skull using screws and dental cement (Jet Repair Acrylic; Lang Dental Manufacturing, Chicago, IL, USA).

Cortical activity recording

Recording sessions began 3-4 days after surgery, to fully recover basal functions such as gait balance and food-intake, and it lasted up to 11 days, based on implant survivor. Before each recording session, the implanted μECoG or intra-cortical array was manually connected to a wireless headstage interfaced with a receiver (W-Series, Triangle Biosystems International, Durham, USA), gently holding the conditioned rats. Through the headstage, signals were amplified × 800 and bandpass filtered between 0.8 and 7000 Hz[67]. Then, signals were elaborated differently based on protocol of recording, namely epidural field potentials or single unit activity.

Epidural field potentials

Signals were further amplified × 10, bandpass filtered between 3 and 250 Hz, digitized with a sampling rate of 2 KHz, and stored for the offline analysis (Visual Basic .NET code and National Instrument library). Averaging of 50-100 trials (usually acquired in 4-7 days), starting 700 ms before and ending 500 ms after the grasping, yielded one evoked potential.

Single neuron activity

Signals were further amplified × 10, digitized with a sampling rate of 30 KHz (Visual Basic .NET code and National Instrument library), and stored for the offline analysis. For spikes detection, the signal was band-passed (300-3000 Hz), thresholded using 3.5 standard deviations (SD) above and below the mean of the sample distribution and extracted waveforms were clustered using K-means Algorithm of Off (Plexon Inc, Greenville, USA).

Electrodes placement reconstruction

At the end of the intracortical recording period, somatosensory evoked potentials (SEPs) were assessed under electrical peripheral stimulation in ketamine-anaesthetized rats, to assess size and location of the forelimb representation with respect to the array position. Animals were in a prone position and the median nerve of the preferred forelimb was stimulated by a WPI A310 pulse generator through a WPI A360R stimulus isolation unit (World Precision Instruments, Sarasota, USA), with a rectangular constant current pulses with a frequency of 0.25 Hz, via bipolar subcutaneous needle electrodes (2 mm separation). Pulse duration was 0.2 ms and amplitude was set at threshold level to evoke a visible forepaw twitch (usually in the 1-2 mA range). Signals were amplified × 10, bandpass filtered between 3 and 250 Hz, digitized with a sampling rate of 2 KHz, and stored for the offline analysis (Visual Basic .NET code and National Instrument library). Averaging of 100 sweeps, starting at stimulus delivery and ending 100 ms after, yielded one SEP.

Histology

At the end of the recording period, each animal was deeply anaesthetised with Zoletil 100 (10 mg/Kg, i.m.; Virbac Laboratories, Carros, France), transcardially perfused with saline at room temperature, and fixed with cold 4% paraformaldehyde at pH 7.4. Brains were removed, post-fixed overnight, and transferred to 30% sucrose solution for cryoprotection until they sunk. A freezing microtome (SM2000R; Leica Microsystems, Wetzlar, Germany) was then used to cut 50 μm coronal sections, which were collected free floating in saline for Nissl staining, according to a previously described protocol[21,65]. Briefly, sections at the level of the motor cortex were mounted on chrome-alum-coated slides, stained with cresyl violet, dried in escalating alcohol concentration, cleared in xylene, coverslipped with mounting medium, and captured using a computer-interfaced light microscopy workstation (Zeiss Axioskop, Carl Zeiss, Jena, Germany) with a high-resolution digital camera (AxioCam ICc3, Carl Zeiss, Jena, Germany). For each section (Figure S3L), electrodes placement was assessed and whole array position reconstructed onto schematic templates of coronal sections[68].

QUANTIFICATION AND STATISTICAL ANALYSIS

Data presentation and statistical analysis

Data are represented as mean ± SEM and were obtained from twelve animals. In the present work, a motor site/neuron was defined as site/neuron significantly modulated by grasping execution, whereas a visuomotor site/neuron as site/neuron significantly modulated by grasping execution and observation. Finally, visual site/neuron refers to a site/neuron significantly modulated by grasping observation. Considering the epidural field potentials, activities were aligned with respect to food touch, averaged among trials, and expressed in function of time, to obtain a profile which provide a continuous time-dependent measure. To ensure that the response at each cortical site was modulated by the task, the difference in the activity was statistically assessed for each site by unpaired Student's t test between two different 300-ms epochs, namely baseline (from 700 to 400 ms before food touch) and action (from 150 ms before and 150 ms after touch). Epoch duration was selected by looking at the temporal evolution of the cortical potentials (usually observed at ~100 ms around touch). Sites showing significant potentials were further taken into consideration. Considering single neuron data, spike trains were aligned with respect to food touch (MATLAB Mathworks, Natick, USA), averaged among trials, and expressed in function of time (20ms bins) to obtain a time-dependent measure of the firing pattern (spike/s). To ensure that the response of a selected neuron was modulated by the task, the difference in activity was statistically assessed for each neuron by repeated-measures one-way ANOVA followed by Dunnett's post hoc test for multiple comparison among three different 300-ms epochs, namely baseline (from 1000 to 700 ms before food touch), pre-touch (from 300 ms before touch to food touch) and post-touch (from touch to 300 ms after touch). Epoch duration was chosen based on the time it takes for the extension or retraction of the forelimb (usually ~250 ms each). Differently from epidural signals, epochs were extended from two to three, since an early and later modulation was expected at the level of single neuron activity. Only neurons showing significant differences with respect to baseline, were further taken into consideration. Neuronal populations and sub-populations were then assessed by two-way repeated-measures ANOVA, with conditions and epoch as factors, followed by Bonferroni post hoc test for multiple comparisons. For both μECoG and intracortical recordings, to characterize the spatial distribution in the motor cortex surface of the task-related activity across animals, a 2D distribution of motor-, visuo-motor and visual sites (for μECoG) or neurons (for intracortical recording) at coordinates relative to the bregma was generated using a spatially interpolated contour plot. Each movement-related site was assigned X and Y values corresponding to the coordinate relative to the bregma (ML and AP, respectively), and a Z value corresponding to the assigned probability. A probability at a given site of 100% will be achieved when all responses of the same group will be detected at that site. A quantitative evaluation of the motor cortex configuration was obtained from the sizes of the activated area, assuming that each task-related site represented a 0.63 mm^2 (0.9 × 0.7 mm) or 0.25 mm^2 (0.5 × 0.5 mm) of cortical surface, based on inter-electrode distance for μECoG or intracortical electrode arrays, respectively. Unpaired Student's t test or one-way ANOVA followed by Dunnett's post hoc test for multiple comparison were used to assess difference among different conditions. P values < 0.05 were considered to be statistically significant. All details on quantitative methods and software used were explained in the Method details section.